2017

Mapping and exploring variation in post-fire vegetation recovery following mixed severity wildfire using airborne LiDAR:

Chris Gordon
University of Wollongong, gordonc@uow.edu.au

Owen F. Price
University of Wollongong, oprice@uow.edu.au

Elizabeth M. Tasker
Department Of The Environment, NSW, etasker@uow.edu.au

Publication Details

Gordon, C. E., Price, O. F. & Tasker, E. M. (2017). Mapping and exploring variation in post-fire vegetation recovery following mixed severity wildfire using airborne LiDAR:. Ecological Applications, 27 (5), 1618-1632.

Mapping and exploring variation in post-fire vegetation recovery following mixed severity wildfire using airborne LiDAR:

Abstract

There is a public perception that large high-severity wildfires decrease biodiversity and increase fire hazard by homogenizing vegetation composition and increasing the cover of mid-story vegetation. But a growing literature suggests that vegetation responses are nuanced. LiDAR technology provides a promising remote sensing tool to test hypotheses about post-fire vegetation regrowth because vegetation cover can be quantified within different height strata at fine scales over large areas. We assess the usefulness of airborne LiDAR data for measuring post-fire mid-story vegetation regrowth over a range of spatial resolutions (10 x 10 m, 30 x 30 m, 50 x 50 m, 100 x 100 m cell size) and investigate the effect of fire severity on regrowth amount and spatial pattern following a mixed severity wildfire in Warrumbungle National Park, Australia. We predicted that recovery would be more vigorous in areas of high fire severity, because park managers observed dense post-fire regrowth in these areas. Moderate to strong positive associations were observed between LiDAR and field surveys of mid-story vegetation cover between 0.5-3.0 m. Thus our LiDAR survey was an apt representation of on-ground vegetation cover. LiDAR-derived mid-story vegetation cover was 22-40% lower in areas of low and moderate than high fire severity. Linear mixed-effects models showed that fire severity was among the strongest biophysical predictors of mid-story vegetation cover irrespective of spatial resolution. However much of the variance associated with these models was unexplained, presumably because soil seed banks varied at finer scales than our LiDAR maps. Dense patches of mid-story vegetation regrowth were small (median size 0.01 ha) and evenly distributed between areas of low, moderate and high fire severity, demonstrating that high-severity fires do not homogenize vegetation cover. Our results are relevant for ecosystem conservation and fire management because they: indicate that native vegetation are responsive and resilient to high-severity fire, and show the usefulness of remote sensing tools such as LiDAR to monitor post-fire vegetation recovery over large areas in situ.

Disciplines

Medicine and Health Sciences | Social and Behavioral Sciences

Publication Details

Gordon, C. E., Price, O. F. & Tasker, E. M. (2017). Mapping and exploring variation in post-fire vegetation recovery following mixed severity wildfire using airborne LiDAR:. Ecological Applications, 27 (5), 1618-1632.

Ecological Applications, 27(5), 2017, pp. 1618–1632

Mapping and exploring variation in post-fire vegetation recovery following mixed severity wildfire using airborne LiDAR

Christopher E. Gordon,[1,3] Owen F. Price,[1] and Elizabeth M. Tasker[2]

[1]*Centre for Environmental Risk Management of Bushfires, University of Wollongong, Wollongong, 2522 New South Wales Australia*
[2]*Science Division, New South Wales Office of Environment and Heritage, 43 Bridge Street, Hurstville, 2220 New South Wales Australia*

Abstract. There is a public perception that large high-severity wildfires decrease biodiversity and increase fire hazard by homogenizing vegetation composition and increasing the cover of mid-story vegetation. But a growing literature suggests that vegetation responses are nuanced. LiDAR technology provides a promising remote sensing tool to test hypotheses about post-fire vegetation regrowth because vegetation cover can be quantified within different height strata at fine scales over large areas. We assess the usefulness of airborne LiDAR data for measuring post-fire mid-story vegetation regrowth over a range of spatial resolutions (10 × 10 m, 30 × 30 m, 50 × 50 m, 100 × 100 m cell size) and investigate the effect of fire severity on regrowth amount and spatial pattern following a mixed severity wildfire in Warrumbungle National Park, Australia. We predicted that recovery would be more vigorous in areas of high fire severity, because park managers observed dense post-fire regrowth in these areas. Moderate to strong positive associations were observed between LiDAR and field surveys of mid-story vegetation cover between 0.5–3.0 m. Thus our LiDAR survey was an apt representation of on-ground vegetation cover. LiDAR-derived mid-story vegetation cover was 22–40% lower in areas of low and moderate than high fire severity. Linear mixed-effects models showed that fire severity was among the strongest biophysical predictors of mid-story vegetation cover irrespective of spatial resolution. However much of the variance associated with these models was unexplained, presumably because soil seed banks varied at finer scales than our LiDAR maps. Dense patches of mid-story vegetation regrowth were small (median size 0.01 ha) and evenly distributed between areas of low, moderate and high fire severity, demonstrating that high-severity fires do not homogenize vegetation cover. Our results are relevant for ecosystem conservation and fire management because they: indicate that native vegetation are responsive and resilient to high-severity fire, and show the usefulness of remote sensing tools such as LiDAR to monitor post-fire vegetation recovery over large areas in situ.

Key words: *Australia; biophysical predictor; fire severity; LiDAR; spatial analysis; vegetation; Warrumbungle National Park; wildfire.*

Introduction

The dramatic consumption and blackening of vegetation by wildfire leads to a public perception that fire is bad for the environment and biodiversity. However, ecological research has revealed a much more nuanced situation, with most species displaying a range of adaptations that enable them to persist in fire-prone environments (i.e., fire stimulates germination and recruitment; Clarke et al. 2015). Also, it is becoming clear that the fire regime (the long-term pattern of fire) is more important than the impact of individual fires (Gill 1975) for the long-term persistence of populations. In recent years, research focus has turned to fire severity because there is growing evidence for considerable variation in the ecological effects among and even within fires. Fire severity is a measure of the biological impact of a fire, usually the amount of vegetation consumed (Keeley 2009). It can be measured in the field or from remote sensing using multi-spectral indices that describe blackening (Hammill and Bradstock 2006). High-severity fires remove more vegetation so they might be expected to have a higher biological impact (Bradstock 2009, Adams and Attiwill 2011). However, there is increasing evidence that some floristic elements are favored by high-severity fires because these fires are required to trigger seed germination (Ooi et al. 2006, Liyanage and Ooi 2015). Also, studies have found that high-severity fires often have minimal effects on vegetation diversity, including in North American pine forests and west coast shrublands (Turner et al. 1999, Purdon et al. 2004, Keeley et al. 2008, Fornwalt and Kaufmann 2014) and Australian eucalypt forests (Bradstock 2009, Knox and Clarke 2012, Camac et al. 2013, Clarke et al. 2014).

In January 2013, a wildfire burned ~90% of the 23,000-ha Warrumbungle National Park in central-western New South Wales, Australia, causing a range of

Manuscript received 19 January 2016; revised 4 January 2017; accepted 3 March 2017. Corresponding Editor: Xiangming Xiao.
[3] E-mails: gordonc@uow.edu.au

significant impacts including a large soil erosion event, significant reduction in koala (*Phascolarctos cinereus*) and brush-tailed rock-wallaby (*Petrogale penicillata*) populations and the destruction of 50 houses near the park boundary (Burned Area Assessment Team 2013; *unpublished government report*). Much of the area was severely burned with total crown consumption, but there were areas of much milder severity that acted as refuges for the biota. Park managers observed widespread vegetation regrowth following the fire and wanted to know the pattern of post-fire recovery in terms of biodiversity value and fuel hazard for future fire regime management.

Here we present a quantification of the spatial pattern of mid-story vegetation regrowth (defined as all vegetation 0.5–3.0 m from the ground) following the fire and statistical modelling of potential reasons why the response varied spatially. This study was used to test two opposing hypotheses about fire severity and vegetation response: (1) high-severity fire causes high biological impact and hence slow recovery (i.e., the public's perception of vegetation response to severe wildfire) or (2) high-severity fire creates the conditions for strong recovery (i.e., fire stimulates germination and recruitment; Ooi et al. 2006, Liyanage and Ooi 2015). Gordon et al. (2017) found widespread vegetation regrowth following the fire (particularly of *Acacia* shrubs, which have long-lived, fire-responsive, soil seed banks), including in areas burned at high severity; *Acacia* cover was 4.3 times greater 2 yr after than before the fire, cover was positively correlated with fire severity and the mean maximum height of recruiting seedlings was 2.4 m. Therefore our main hypothesis was that recovery would be more vigorous in areas of high fire severity. Moreover, we expected patches of vigorous regrowth to be large (several hectares), reflecting the size of the high-severity patches (85% of the high-severity fire occurred within discrete patches >10 ha in area). Such large areas of dense regrowth could pose a significant fire hazard in the park, which was something that park managers were particularly concerned about both in the short and long term. As well as the ecological aspects, this study tests the use of airborne LiDAR technology to map post-fire vegetation recovery, a technique that could be used routinely if it is found to be accurate and precise. While airborne LiDAR data has been applied to measure many aspects of vegetation structure (especially in forests; Gonzalez-Olabarria et al. 2012, Levick et al. 2012, Brosofske et al. 2014, Harpold et al. 2015), its use to map post-fire vegetation recovery across large areas, especially in Australia, is rare (Kane et al. 2013, 2014).

Methods

Study area

The study was conducted in Warrumbungle National Park (31.29° S, 149.01° E) ~10 km west of Coonabarabran in central-western New South Wales, Australia (Fig. 1). The park is typified by a topographically diverse landscape with steep volcanic mountains rising to 1,206 m above sea level and sandstone river flats laying 400–500 m above sea level. Average annual rainfall at Coonabarabran, the closest long-term weather station to the park, is 750.7 mm (134 yr of data; Australian Bureau of Meteorology). Rainfall decreases east-west due to orographic effects of the mountain range. Prior to the 2013 wildfire, most of the park (~70%) had been unburned since at least 1968. The vegetation of the park is dominated by woodland and open forests with trees comprising white box (*Eucalyptus albens*), yellow box (*E. melliodora*), iron bark (*E. crebra*), red scribbly bark (*E. macrorhyncha*), rough barked apple (*Angophora floribunda*), white cyprus (*Callitris glaucophylla*), black cyprus (*C. endlicheri*), and bloodwood (*Corymbia dolichocarpa*). Minor areas of the park are dominated by Motherumbah shrublands (*Acacia cheelii*; 10% area) or grasslands (*Austrostipa* spp., *Echium plantagineum*, or *Microlaena stipoides*; 3% area).

The 2013 wildfire ignited from an unknown cause on the evening of 12 January. It escaped containment lines early on 13 January and spread 21 km to the east under extreme fire weather (39°C temperatures, <20% humidity, wind speeds of ~40 km/h, Forest Fire Danger Index of 60; data from Siding Spring Observatory [Australian Bureau of Meteorology 2016]) until the night when conditions eased. It continued to burn for several more days, mainly spreading south. The final area burned by the fire was 45,000 ha, including ~90% of the park (Fig. 1). The percentage of area burned by low- (canopy unburned, understory scorched or consumed), moderate- (canopy scorched, understory consumed), and high- (all canopy consumed) severity fire was 21%, 42%, and 37%, respectively (Price and Storey 2015; *unpublished government report*).

LiDAR data

The New South Wales Department of Land and Property Information conducted a LiDAR survey of Warrumbungle National Park between 3 and 11 September 2014, ~20 months after the wildfire. LiDAR data was collected using a Leica ALS50-II airborne sensor (Leica Geosystems, Heerbrugg, Switzerland) with an average flight height of 2,801 m, a swath width of 737 m, and a scan angle of −17° to 22°. Data consisted of 100 2 × 2 km Las file "tiles" representing the first four returns of the LiDAR laser beam. The average point cloud density was 1.01 points/m^2 and the maximum point cloud density was 1.59 points/m^2, respectively. The LiDAR vendor reported the vertical and horizontal accuracy of the LiDAR data as 30 and 80 cm, respectively.

LiDAR processing

The percentage of mid-story vegetation cover between 0.5–3.0 m was assessed at four spatial resolutions (10 × 10 m, 30 × 30 m, 50 × 50 m, 100 × 100 m) in areas burned by the 2013 wildfire. We chose to assess

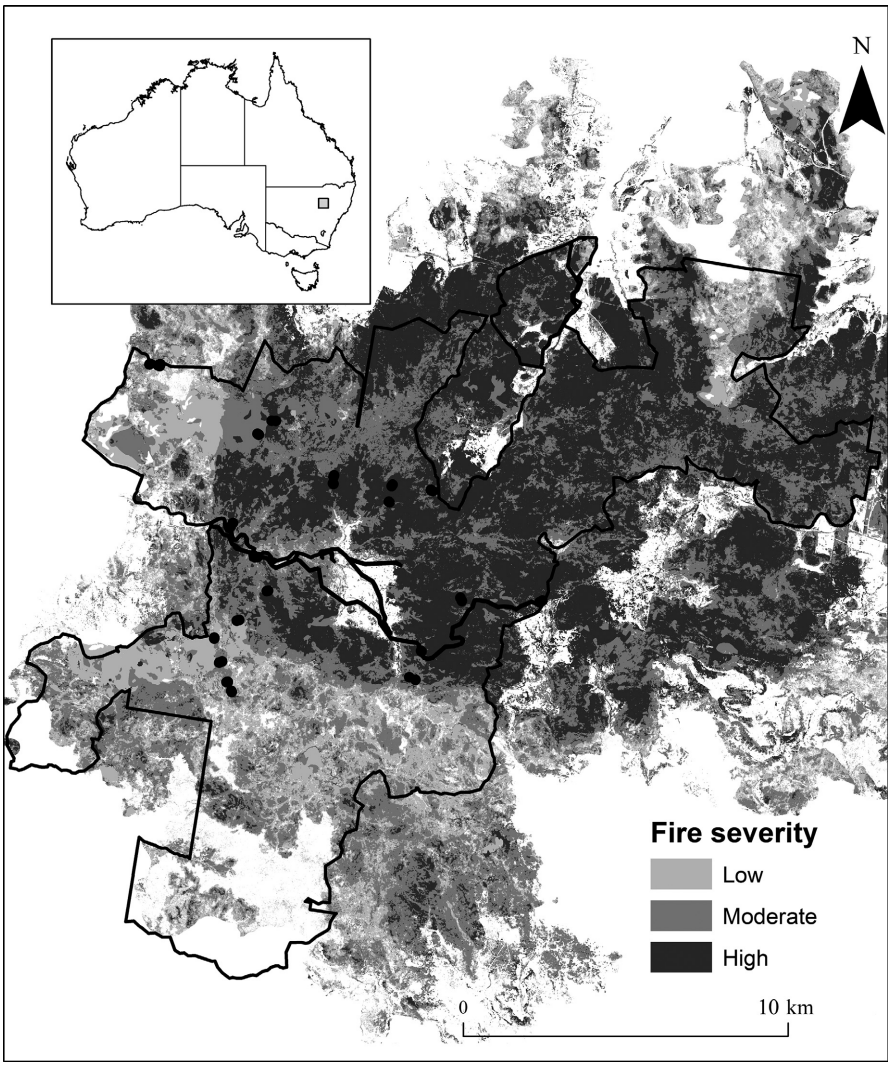

FIG. 1. Map of Warrumbungle National Park showing fire severity during the 2013 wildfire and the location of 40 field sites (black circles) used to validate our LiDAR survey. The insert map shows the location of the park (gray) in Australia.

mid-story vegetation cover within this height strata because (1) field surveys showed vegetation regrowth typically occurred <3 m from the ground (an average maximum regrowth height of 2.43 ± 0.14 m [mean ± SE] was observed at 60 field sites surveyed ~2 yr after the wildfire; *unpublished data*), and (2) LiDAR ground models are generally accurate to ~±0.25 m and trying to measure vegetation too closely to this error range can result in vegetation measurement errors (Dubayah and Drake 2000, Mitchard et al. 2012). The four spatial resolutions were chosen to investigate scale-dependent relationships between mid-story vegetation cover and important predictors of cover (see *Predictors of mid-story vegetation cover* section).

LiDAR files were converted to height above the ground and LiDAR points that were classified as buildings or located in rocky outcrop areas were excluded using the vendor-identified buildings classification of the LiDAR data and a rock mask raster map created as part of the fire severity mapping (see *Predictors of mid-story vegetation cover* section). The number of LiDAR point returns in each cell were then summed between 0.5–3.0 m (i.e., mid-story vegetation) and 0–3 m (i.e., the entire mid-story vegetation canopy including ground points), and percentage of mid-story vegetation cover was calculated as all 0.5–3.0 m point returns divided by 0–3 m point returns multiplied by 100. A technical description of the LiDAR survey method is described in Appendix S1: Box S1.

Field validation of the LiDAR survey

A point-intersect method was used to gather field cover data to validate LiDAR mid-story vegetation cover at 40 20 × 20 m area sites (Fig. 1). To ensure that field sites sampled a range of vegetation densities, one low- and one high-density vegetation site (densities

assessed visually) was sampled 40–200 m apart at 20 locations. At each site, a 20 × 20 m plot was marked using measuring tapes. A Bosch 250 VF professional rangefinder (Bosch, Stuttgart, Germany) placed at the end of a 0.5 m tripod with the laser pointing toward the sky was then used to measure the distance to overlying vegetation at 36 points spaced at 4-m intervals. Vegetation cover was then calculated as the percentage of the 36 points intersecting overlying vegetation between 0.5–3.0 m above the ground. Pilot study work showed that 36 points reliably estimated mid-story vegetation cover (*unpublished data*). The location of the center of each site was measured using a recreational grade GPS (Garmin GPS 60, Garmin Ltd., Schaffhausen, Switzerland). The field survey was conducted in August 2015, 11 months after the LiDAR survey.

Linear models were used to test the precision and accuracy of LiDAR mid-story vegetation cover using the 10 × 10 m and 30 × 30 m cell resolution maps; these spatial resolutions most closely resembled the size of the field plot. The recreational grade GPS used to mark field sites reported a spatial error of up to 10 m. To explore if this error influenced our result, we offset the location of the field sites by 5 and 10 m to the east, then reassessed associations between field and LiDAR cover using separate linear models.

Predictors of mid-story vegetation cover

A random sample of 3,008 cells sampled within the perimeter of the 2013 wildfire was used to test the relative effects of 12 predictor variables on mid-story vegetation cover between 0.5–3.0 m. Cells were separated by at least 250 m. Predictor variables were chosen based on a priori knowledge of processes thought to influence vegetation regrowth following fire (Table 1).

Topography can affect vegetation recovery in a variety of ways, including influencing the microclimate, erosion, soil depth and moisture content, and sun exposure. A 5-m resolution Digital Elevation Model (DEM) obtained from the New South Wales Office of Environment and Heritage was used to calculate elevation, slope, aspect, and solar radiation on the 2013 summer and winter solstice days. The solar radiation metric used the hemispherical view-shed algorithm (Rich et al. 1994, Fu and Rich 2002) to measure the amount of solar insolation ($W \cdot h^{-1} \cdot m^{-2}$) on summer and winter solstice days during 2013, given elevation, slope, aspect, and latitude inputs. Solar radiation was measured on solstice days to maximize the difference in solar radiation between summer and winter periods.

The Compound Topographic Index (CTI) is a steady-state wetness index that measures the cumulative upstream/upslope contribution of cells to other cells. High CTI values are associated with flat low-lying areas, whereas low CTI values are associated with steep upslope areas. CTI is highly correlated with several soil attributes important for vegetation growth such as soil depth, silt percentage, organic matter content, and phosphorous (Moore et al. 1993, Gessler et al. 1995). Eq. 1 shows that CTI is proportional to slope, upstream/upslope contribution, and orthogonal flow direction

$$\mathrm{CTI} = \frac{(\text{flow accumulation}(\text{flow index to each cell}) + 1) \times \text{pixel area(m)}}{\mathrm{TAN}(\text{slope(radiuns)})} \quad (1)$$

Fire severity and time-since-fire (here defined as the interval between the 2013 wildfire and the previous fire) can impact post-fire vegetation recovery by reducing or promoting the abundance of some but not other species (Bradstock et al. 2002). A fire-severity map for the 2013 wildfire was created (Price and Storey 2015; *unpublished government report*) using the relativized differenced Normalized Difference Vegetation Index (NDVI; Miller and Thode 2007) from two 5-m resolution Rapideye satellite images obtained before and after the fire (29 December 2012 and 24 January 2013). NDVI measures the "greenness" of vegetation, and the comparison of before and after images essentially measures the loss of greenness or the degree of blackening. The relativizing weights the severity values by the pre-fire NDVI to correct bias toward less vegetated areas. Areas affected by cloud in either image were excluded, as was bare rock (as identified by image classification of 50-cm resolution pre-fire aerial photography). The values were converted into a severity classification (0, unburned; 1, understorey burned but not the crown canopy; 2, crown scorch; 3, crown consumption), using 28 ground points (Burned Area Assessment Team 2013; *unpublished government report*) and 54 points identified from oblique aerial photography (with 94% accuracy). Remote sensed severity mapping can distinguish crown and understorey consumption in Eucalypt forests because the tree canopy is usually <30% (Hammill and Bradstock 2006). In Warrumbungle National Park, our LiDAR data suggested that mean canopy cover between 3 and 20 m was 44% (this value was calculated from a sample of 50 cells unburned by the 2013 wildfire using the upper canopy cover map described below; see *Predictors of mid-story vegetation cover* section).

Time-since-fire was sampled at a 50-m cell resolution using a fire history map provided by the New South Wales Office of Environment and Heritage. This map was created using a combination of satellite imagery, aerial photographs, and field observations.

To test whether the pre-fire biota influenced vegetation recovery, a 1:50,000 scale vegetation community map was obtained from the New South Wales Office of Environment and Heritage (Hunter 2008; *unpublished government report*). The vegetation map showed nine dominant vegetation communities (Appendix S1: Table S1). Following preliminary analysis of our LiDAR cover maps, we simplified these into four classes dominated by *Eucalyptus* spp. (vegetation communities C1, C3, C4, C7), *Acacia* spp. (vegetation communities C8 and C9), *Callitris* spp. (vegetation community C2), and

TABLE 1. Predictor variables included in linear mixed-effects models and their hypothesized effects on mid-story vegetation cover in areas of Warrumbungle National Park burned by the 2013 wildfire.

Predictor variable	Predicted response of mid-story vegetation cover	Description	Units
Elevation	negative due to lower temperature and hence growth at high elevations	meters above sea level	m
Slope	negative due to higher soil erosion, soil nutrients, and lower water availability on high incline areas	degree of incline	degrees
Aspect	lower on north and east facing slopes due to lower water availability	bearing of slope face	Degrees
Solar Radiation: summer solstice day	negative due to lower water availability on north and east facing slopes	solar radiation during the 2013 summer solstice day	$W{\cdot}h^{-1}{\cdot}m^{-2}$
Solar radiation: winter solstice day	positive due to lower water availability on north and east facing slopes	solar radiation during the 2013 winter solstice day	$W{\cdot}h^{-1}{\cdot}m^{-2}$
Compound topographic index	positive due to higher levels of soil and soil nutrient accumulation in low elevation areas	steady state wetness index	CTI
Time-since-fire	negative due to removal of the soil seed bank of pyrophobic species in recently burned areas	time-since-fire prior to the 2013 wildfire	yr
Fire severity	positive due to vigorous regrowth of pyrophilic *Acacia* spp. in areas of high fire severity	index of fire severity: low, moderate or high	three-factor categorical variable
Easting	positive due to a decreasing east-west rainfall gradient influencing water availability	east-west spatial location	UTME
Upper canopy cover	negative due to increased competition in areas of dense overstory canopy cover	vegetation cover between 3 and 20 m	%
Vegetation type	highest regrowth in areas dominated by *Acacia* communities and lowest in areas dominated by grassland communities	dominant vegetation: *Acacia* spp., *Eucalyptus* spp., *Callitrus* spp., or grasses	four-factor categorical variable
Geology type	highest regrowth on nutrient rich basalt soils	underlying geology: basalt or sandstone	two-factor categorical variable

grasslands (vegetation communities C5 and C6; see Appendix S1: Table S1 for a description of the vegetation community names used here).

To test whether underlying geology and hence productivity influenced vegetation recovery, a 1:250,000 scale geology map was obtained from the New South Wales Office of Environment and Heritage. Four geology classes were present at our subsample of 3,008 cells: undifferentiated basalts, Pilliga sandstones, Keelindi beds sandstones, and Purlawaugh Foundation sandstones. Following preliminary analysis, we grouped all three sandstone classes into one, resulting in a simple sandstone/basalt geology classification.

There is a considerable east-west rainfall gradient across the park, due to orographic effects of the mountains intercepting rainfall, which predominantly arrives with easterly winds. There is no actual data on rainfall patterns across the park, so we used geographic easting as a surrogate for this gradient.

Overstory vegetation (i.e., upper canopy cover) can potentially impact mid-story vegetation regrowth via competition or facilitation effects (Bazzaz 1996). The LiDAR survey was used to assess upper canopy cover, which is here defined as all vegetation falling between 3 and 20 m from the ground. The LiDAR data was processed using the methods described in the *LiDAR processing* section and Appendix S1: Box S1. Cover was calculated as the sum of all point returns between 3 and 20 m divided by the sum of all point returns between 0–20 m multiplied by 100.

Linear mixed-effects models were used to identify which of the 12 predictor variables best explained mid-story vegetation cover at each spatial resolution. Continuous predictor variables were sampled at the same spatial resolution as mid-story vegetation cover for each analysis and categorical predictor variables and easting were sampled at the central point of each replicate cell. Fire severity was categorized at each spatial resolution by summing all 5-m resolution low-, moderate-, and high-severity cells falling within a larger cell size and using the most frequently observed category. Where tied values occurred, the higher severity category was used. Mid-story vegetation cover was log + 1 transformed prior to analysis to normalize data. Although our sample points were evenly distributed throughout the park, it was possible that spatial location may have influenced trends in mid-story vegetation cover. For example, high-severity fire may be an important predictor of mid-story vegetation cover, however high-severity fire may have been limited to one spatial area. To account for spatial confounding in our models, drainage watershed (i.e., drainage basin) was included as a random factor in all linear mixed-effects models. A drainage watershed map created in ArcMAP 10.2 using the DEM as an input identified 34 discrete watersheds within and surrounding the park (watershed area 12.21 $\pm$ 1.52 km^2 [mean $\pm$ SE]).

Prior to model fitting, Pearson's correlation tests were used to identify collinearity between continuous predictor variables (collinearity of predictor variables can lead to irregular behavior of mixed-effects models; Zuur et al. 2009). If any two predictor variables had a correlation coefficient > 0.7, they were deemed to be proxies of one another and one was removed. All possible combinations of predictor variables were then computed using the dredge function in the MuMIN package (Barton 2011) in the program R (R Development Core Team 2013). Models were ranked based on Akaike Information Criterion (AIC; the best model was that with the lowest AIC value) and an Akaike weight (w_i; the likelihood that a model is true given a subset of competing models) was calculated. A best subset of models was then determined by summing w_i values, starting with the model with the highest w_i and continuing in decreasing order until the Σw_i values reached 0.95 (Burnham and Anderson 2003). Within this subset of models, the relative importance of each predictor variable was assessed by summing w_i values for all models within which a predictor variable occurred (Burnham and Anderson 2003). A relative importance value of 1 implies that a predictor variable is present in all models and a value of 0 implies that a predictor variable is present in no models. Marginal (inclusive of fixed effects only) and condition (inclusive of fixed and random effects) R^2 values were calculated and used to determine the goodness-of-fit for all models using the method described in Nakagawa and Schielzeth (2013).

Spatial clumping of mid-story vegetation patches

To compare the size and spatial clumping of vegetation recovery between areas of low-, moderate-, and high-fire severities, we created maps of dense vegetation patches using the 0.5–3.0 m LiDAR mid-story vegetation cover map sampled at a 10 $\times$ 10 m cell resolution. We defined "dense" vegetation to be any 10 $\times$ 10 m cell above the 66th percentile value of LiDAR cover cells (i.e., >20%). We aggregated all dense cover cells sharing a straight edge into discrete patches and calculated the area (ha) of each discrete patch. Finally, we extracted all patches in low, moderate, and high fire severity areas and constructed plots of cumulative patch occurrence against patch area. Kolmogorov-Smirnov tests were used to compare the distribution of cumulative patch area between low, moderate, and high fire severity areas.

The Getis-Ord test statistic was used to test for spatial clustering of dense mid-story vegetation cover patches in ArcGIS 10.2 (Getis and Ord 1992, Ord and Getis 1995). The Getis-Ord test statistic uses a neighborhood distance matrix (500 m for our analysis) to identify "hotspots," where large area patches are grouped around other large area patches, and "coldspots," where small area patches are grouped around other small area patches. The statistical significance of hotspot and coldspot patch clumping was assessed using z and P values, and the degree of statistical strength was inferred by setting α at 0.1 (90%

confidence level), 0.05 (95% confidence level), and 0.01 (99% confidence level). A non-significant result in the analysis is indicative of no spatial clustering.

Results

LiDAR cover maps

The LiDAR surveys showed a complex pattern of mid-story vegetation cover across the park, including many areas with ≤5% cover (e.g., 45% of cells for the 10 × 10 m resolution map) and few areas with cover ≥30% (e.g., 4% of cells for the 10 × 10 m resolution map; Fig. 2 and Appendix S1: Fig. S1). Moderate to strong positive correlations (R = 0.53–0.87) were observed between the LiDAR maps sampled at different spatial resolution (Appendix S1: Table S2).

Field validation of the LiDAR survey

Moderately strong positive correlations were observed between field surveyed mid-story vegetation cover and LiDAR surveyed cover at the 10-m (R^2 = 0.48) and 30-m (R^2 = 0.56) cell resolutions (Fig. 3a, d). Offsetting the field survey points by 5 and 10 m resulted in a small reduction in R^2 values (Fig. 3). Both the 10- and 30-m resolution LiDAR survey's underestimated mid-story vegetation cover relative to the field survey.

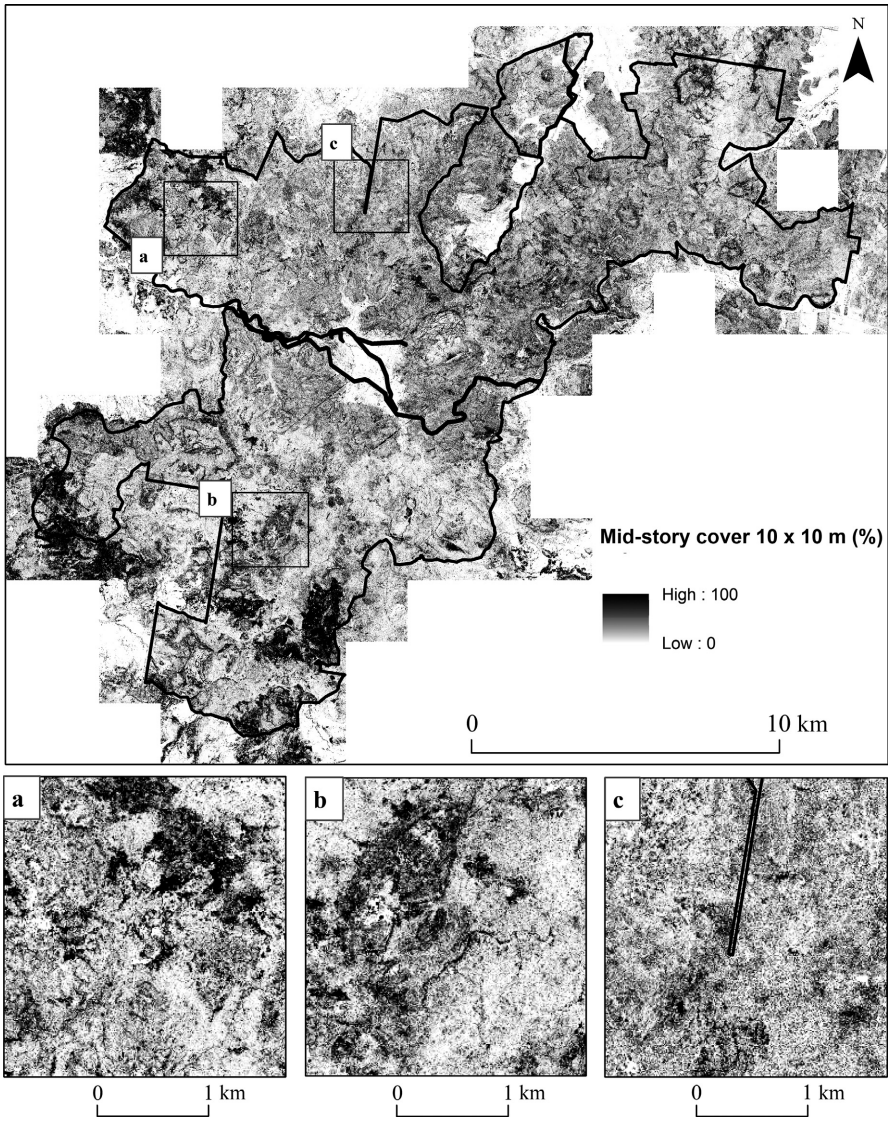

Fig. 2. An example of a LiDAR map showing the percentage of mid-story vegetation cover between 0.5–3.0 m in Warrumbungle National Park. Data was sampled at a 10 × 10 m cell resolution. (a) and (b) show magnified areas of high mid-story vegetation cover and (c) shows a magnified area of low mid-story vegetation cover. The black line shows the boundary of the park.

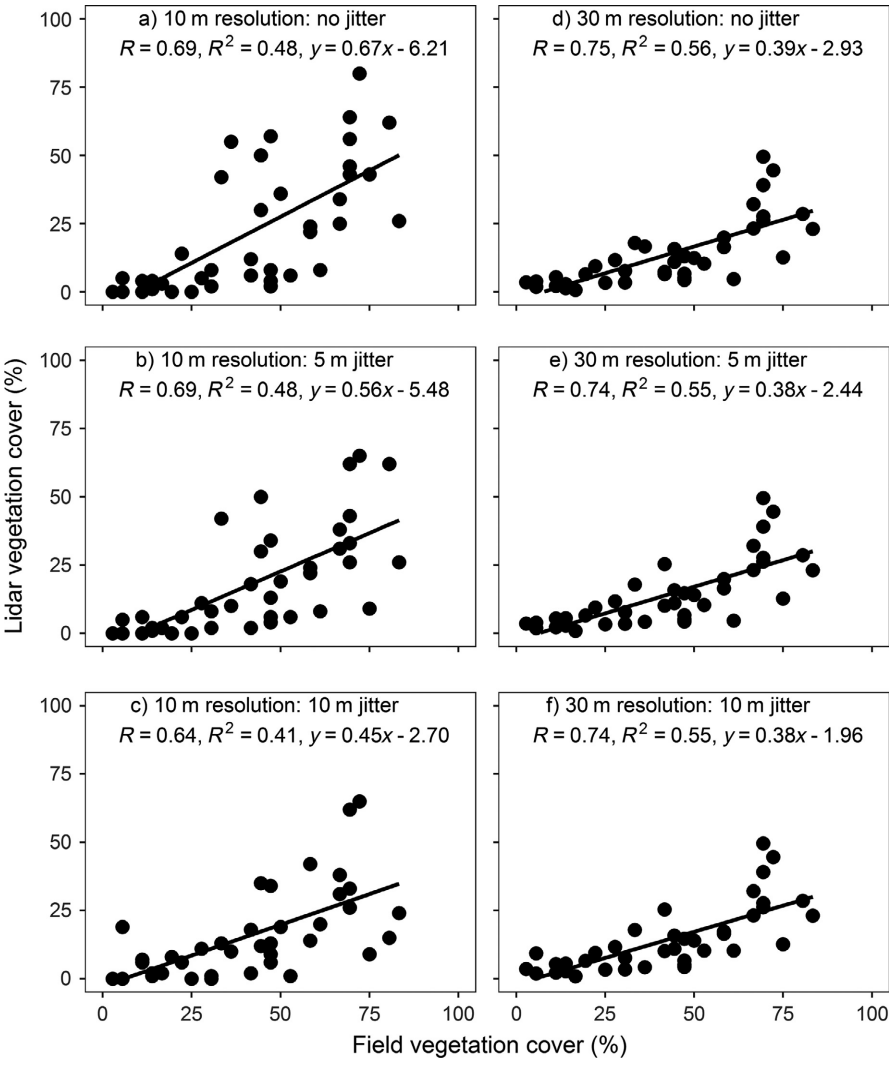

FIG. 3. Scatter plots showing associations between LiDAR and field surveys mid-story vegetation cover (0.5–3.0 m) at 40 sites burned by the 2013 wildfire. LiDAR cover was assessed at a 10 m (a–c) and 30 m (d–f) cell resolution and field survey points were sampled at the GPS location (a and d; no jitter), 5 m east of the GPS location (b and e; 5 m jitter) and 10 m east of the GPS location (c and f; 10 m jitter). Results of linear models between LiDAR and field surveyed vegetation cover are shown for each plot. R represents the Pearson's correlation coefficient, R^2 represents the coefficient of determination and the form of the each linear model is also shown.

Important predictors of mid-story vegetation cover

Fire severity was among the most important predictor of mid-story vegetation cover at each of the four spatial resolutions (Table 2, Fig. 4). At the finest spatial resolution (10 × 10 m), mid-story vegetation cover was 40% greater in areas of high than moderate fire severity, 31% greater in areas of high than low fire severity, and 7% greater in areas of low than moderate fire severity (Fig. 4). At the coarsest spatial resolution (100 × 100 m), mid-story vegetation cover was 31% greater in areas of high than moderate fire severity, 22% greater in areas of high than low fire severity, and 12% greater in area of low than moderate fire severity (Fig. 4).

Low to moderate levels of collinearity were observed between most continuous predictor variables in our linear mixed-effects models (Appendix S1: Table S3). However strong correlations were observed between slope and solar radiation on the 2013 summer solstice day at all spatial resolutions (10 × 10 m, $R = -0.92$; 30 × 30 m, 50 × 50 m, and 100 × 100 m, $R = -0.93$) and slope and the compound topographic index at the 50 × 50 m ($R = -0.75$) and 100 × 100 m resolutions ($R = -0.82$). Because of these strong correlations, slope was excluded from all models.

A low level of model uncertainty was present at each spatial resolution, with three to eight models falling within the 95% confidence sets (Table 2). Elevation

TABLE 2. The best subsets ($\sum w_i = 0.95$) of linear mixed-effects models describing mid-story vegetation regrowth following the 2013 wildfire.

Model parameters													R^2	
CTI	UTME	Elevation	Fire severity	Geology	SR summer	SR winter	TSF	Canopy cover	Vegetation	AIC	ΔAIC	w_i	Mar	Con
10 × 10 m														
		+	+		+			+		8,316.13	0.00	0.43	0.11	0.15
		+	+		+		+	+		8,317.64	1.51	0.20	0.11	0.15
		+	+		+			+	+	8,318.90	2.77	0.11	0.11	0.17
		+	+		+		+	+	+	8,319.66	3.53	0.08	0.12	0.17
		+	+		+					8,320.46	4.33	0.05	0.10	0.15
		+	+		+		+			8,321.29	5.16	0.04	0.11	0.16
		+	+	+	+			+		8,321.51	5.38	0.03	0.11	0.15
		+	+	+	+		+	+		8,322.92	6.79	0.01	0.11	0.16
30 × 30 m														
		+	+		+			+	+	5,667.38	0.00	0.26	0.18	0.30
+		+	+		+			+	+	5,667.56	0.18	0.23	0.18	0.30
		+	+		+		+	+	+	5,668.64	1.26	0.14	0.19	0.30
+		+	+		+		+	+	+	5,668.70	1.32	0.13	0.19	0.31
		+	+	+	+			+	+	5,670.28	2.90	0.06	0.18	0.29
+		+	+	+	+			+	+	5,670.34	2.96	0.06	0.19	0.30
		+	+	+	+		+	+	+	5,671.30	3.92	0.04	0.18	0.30
50 × 50 m														
+		+	+	+	+		+	+	+	4,700.66	0.00	0.55	0.25	0.39
		+	+	+	+		+	+	+	4,701.81	1.15	0.30	0.25	0.39
+		+	+		+		+	+	+	4,704.82	4.16	0.07	0.25	0.40
100 ×														
	+	+	+	+	+		+	+	+	3,791.19	0.00	0.38	0.27	0.39
	+	+	+		+		+	+	+	3,791.93	0.74	0.25	0.27	0.39
		+	+	+	+		+	+	+	3,792.56	1.37	0.19	0.26	0.44
+	+	+	+	+	+		+	+	+	3,794.93	3.74	0.06	0.27	0.39
		+	+		+		+	+	+	3,795.87	4.68	0.04	0.26	0.45
+	+	+	+		+		+	+	+	3,796.48	5.29	0.03	0.27	0.40

Notes: Mid-story vegetation cover was assessed using LiDAR at four spatial resolutions: 10 × 10 m, 30 × 30 m, 50 × 50 m, and 100 × 100 m. AIC, Akaike Information Criterion; ΔAIC, change in Akaike Information Criterion value relative to the best model; w_i, Akaike weight; R^2, marginal (Mar) and condition (Con) R^2 value; CTI, compound topographic index; SR, solar radiation; TSF, time-since-fire; UTME, easting.

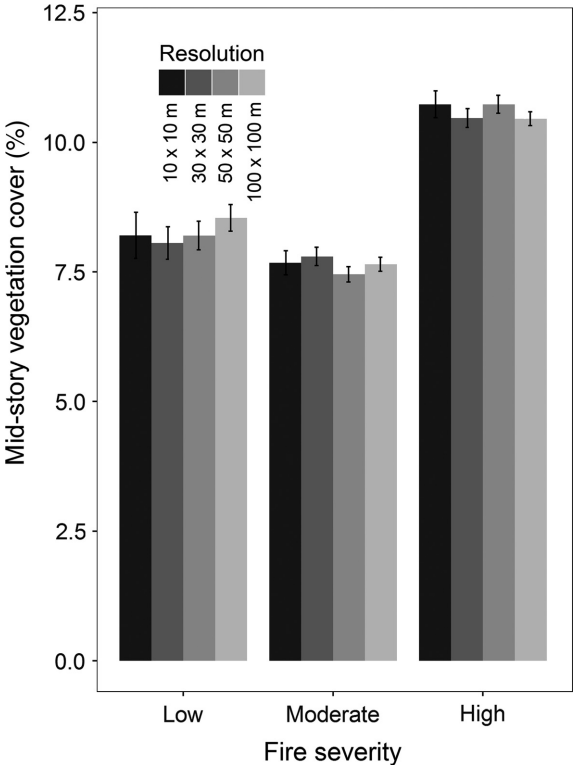

FIG. 4. Mid-story vegetation cover between 0.5–3.0 m (mean ± SE) in areas of low, moderate, and high fire severity. Mid-story vegetation cover was assessed at four spatial resolutions: 10 × 10 m, 30 × 30 m, 50 × 50 m, and 100 × 100 m cell size.

(positive), fire severity (cover greater at high >low >moderate severities), solar radiation on the summer solstice day (positive), and upper canopy cover (negative) were among the strongest predictors of mid-story vegetation cover at all spatial resolutions (w_i = 0.9–1.0); vegetation type (cover greater at *Acacia* > *Callitris* > *Eucalyptus* > grassland areas) was among the strongest predictors at the 30 × 30 m, 50 × 50 m, and 100 × 100 m resolutions; geology (cover greater at volcanic > sedimentary areas) was among the strong predictor at the 50 × 50 m resolution; and time-since-fire (positive) was among the strongest predictors at the 50 × 50 m and 100 × 100 m resolutions (Table 3). Aspect and solar radiation on the winter solstice day were poor predictors of mid-story vegetation cover at all spatial resolutions and the compound topographic index and easting were poor predictors of mid-story vegetation cover at most spatial resolutions (Tables 2, 3).

Marginal and conditional R^2 values were higher at the coarser than finer spatial resolution, however, they never exceeded 0.27 and 0.45, respectively (Table 2). This suggests that the 12 predictor variables and the watershed random factor explained <45% of the variance in mid-story vegetation cover, irrespective of spatial resolution.

Spatial clumping of dense mid-story vegetation

The distribution of dense patch areas were statistically different between areas of low and moderate (D = 0.0.064, P < 0.0001), low and high (D = 0.029, P < 0.0001), and moderate and high fire severity (D = 0.035, P < 0.0001; Fig. 5). A 48.93% portion of dense patches in areas of low fire severity were <0.05 ha in size, 8.62% of dense patches were ≥1 ha, and the largest dense patch was 13.3 ha; 65.32% of dense patches in areas of moderate fire severity were <0.05 ha in size, 1.48% of dense patches were ≥1 ha, and the largest dense patch was 2.77 ha; 47.42% of dense patches in areas of high fire severity were <0.05 ha in size, 12.94% of dense patches were ≥1 ha in size, and the largest dense patch was 10.89 ha.

The Getis-Ord test statistic showed that 87% of polygons (size 0.02 ± 0.06 ha [mean ± SD]) were randomly distributed throughout the 2013 wildfire burn area; i.e., a non-significant Getis-Ord statistic (Fig. 6). One percent of small polygons were clumped around other small polygons at the 90% confidence level (0.015 ± 0.020 ha) and none were clumped around other small polygons at the 95% or 99% confidence levels (Fig. 6). Two percent, 3%, and 7% of large polygons were clumped around other large polygons at the 90% (0.043 ± 0.159 ha), 95% (0.045 ± 0.176 ha), and 99% (0.062 ± 0.398 ha) confidence levels, respectively (Fig. 6).

DISCUSSION

Spatial pattern of mid-story regrowth

Mid-story vegetation recovery was vigorous across widespread areas of the fire including in areas burned with differing severity. The density of regrowth was higher in severely than mildly burned areas irrespective of the spatial resolution of the LiDAR vegetation map. Therefore our main hypothesis was accepted: high-severity fire creates the conditions for strong vegetation recovery. A concurrent study by Gordon et al. (2017) showed that most of the vegetation regrowth was from *Acacia* species with a long-lived fire responsive soil seed bank, and that *Acacia* regrowth amount was positively associated with fire severities. Given this, and the fact that many *Acacia* species have physically dormant seeds that require severe fire to cue germination (Liyanage and Ooi 2015), it is likely that seed dormancy and soil seed bank longevity were important processes facilitating the strong post-fire response reported here, especially in areas burned at high fire severities. Although removal of soil inhibitory effects may also have played some role (Purdie 1977), and more importantly the strong effect of overstory canopy cover in our statistical models (the loss of which is directly related to fire severity) suggests that competition for resources (lower where overstory cover is low) was at least as important a biological driver as fire stimulation of seed germination. Murphy et al. (2015) similarly suggest that competition for resources

TABLE 3. Coefficient estimates (CE) and relative contribution scores (RI) for predictor variables falling within the 95% confidence set ($\sum w_i = 0.95$) of linear mixed-effects models describing spatial trends in mid-story vegetation cover at four spatial resolutions: 10 × 10 m, 30 × 30 m, 50 × 50 m, and 100 × 100 m.

	10 × 10 m		30 × 30 m		50 × 50 m		100 × 100 m	
Variable	CE	RI	CE	RI	CE	RI	CE	RI
CTI	—	—	0.0170	0.46	0.0312	0.67	0.0032	0.09
Easting	—	—	—	—	—	—	<−0.0001	0.76
Elevation	0.0014	1	0.0010	1	0.0011	1	0.0012	1
Fire severity								
Low	−0.4214	1	−0.2626	1	−0.1708	1	−0.1208	1
Moderate	−0.3043	—	−0.2132	—	−0.2104	—	−0.1798	—
High	ref	—	ref	—	ref	—	ref	—
Geology								
Sedimentary	ref	—	ref	—	ref	—	ref	—
Volcanic	0.0014	0.05	0.0144	0.18	0.1102	0.93	0.0609	0.66
SR: summer	−0.0005	1	−0.0004	1	−0.0005	1	−0.0005	1
Time-since-fire	0.0016	0.35	0.0011	0.33	0.0037	1	0.0031	1
Upper canopy cover	−0.0053	0.91	−0.0081	1	−0.0123	1	−0.0127	1
Vegetation								
Acacia	0.0702	0.19	0.3977	1	0.4320	—	0.3426	—
Callitrus	0.0747	—	0.4587	—	0.3858	—	0.3306	—
Eucalyptus	0.0726	—	0.4116	—	0.3489	—	0.2441	—
Grassland	ref	—	ref	—	ref	—	ref	—

Notes: The abbreviation ref represents the reference group for categorical variables —shows the variables not included in the 95% confidence set. CTI, compound topographic index; SR, solar radiation

has a stronger influence than fire itself in structuring eucalypt communities.

Although fire severity was an important predictor of mid-story vegetation in our statistical models, its effect was not as great as what could have been expected given the extent and severity of the fire; mid-story cover was 31% and 40% higher in areas burned at high rather than low or moderate severities, respectively. Our LiDAR survey was conducted ~20 months after the fire, and given this, it is probable that much of the vegetation regrowth was still occurring at the time of the LiDAR survey. Gordon et al.'s (2017) field survey of the park, which was conducted 27–32 months after the 2013 wildfire, showed that mid-story cover was ~70% and 40% higher in areas burned by high rather than low or moderate severity fire, respectively. Collectively with our study, this result suggest that the effects of fire severity on vegetation regrowth increase with time-since-fire till at least and potentially beyond 32 months post-fire.

Contrary to our initial prediction, mid-story vegetation cover was lowest at the moderate- (and not low-) fire severity category (Fig. 4) and most dense vegetation patches were small (0.01 ha) in these areas (Figs. 5, 6). By definition, low-severity fires consume some but not all mid-story vegetation whereas moderate-severity fires consume or scorch the entire mid-story vegetation stratum (Keeley 2009). Given this, more unburned vegetation would have remained in areas of low- rather than moderate-severity fire, and this would have influenced our LiDAR cover values.

Although we observed a significant effect of fire severity on vegetation regrowth amount, other biophysical factors were equally important and the majority of variance in the linear mixed-effects models was unexplained, especially at the smaller spatial resolution (10 × 10 m). Further to this, the regrowth of mid-story vegetation was patchy and most patches were much smaller than patches of similar fire severity. These factors make it difficult to explain the spatial pattern of recovery. Why should one plot have experienced vigorous regrowth while a second with a similar environment and only 10 m from the first have relatively weak regrowth? To some degree, this is likely to be because the content of the seed bank varies according to the past fire regimes and edaphic characteristics of the site (Tozer and Bradstock 2003), in ways that are not correlated by the environmental variables we explored. For example, vigorous growth of the common shrub *Acacia penninervis* at one site may be because the sequence of previous fires lead to a particularly large seed bank, while at another site either the past fires or site factors, such as soil depth or micro-scale nutrient levels, lead to a smaller seed bank or lower growth following the 2013 wildfire. The seed bank is not well described by vegetation mapping because mapping is strongly based on the dominant overstory species, and to a lesser extent on the floristic composition of species present above-ground at the time of mapping. Depending on the post-fire age of the sites at the time of mapping, a significant number of species may not be present above ground or only present in very low numbers. Another possible reason for the weak models is that our model of erosion potential (i.e., Compound Topographic

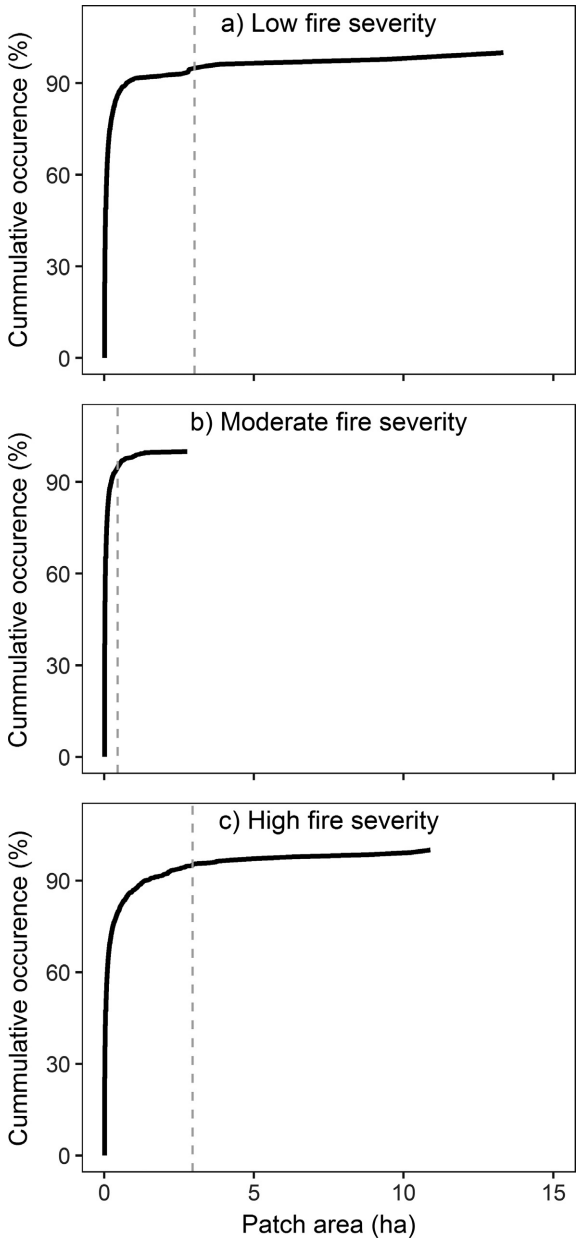

FIG. 5. Plots showing the cumulative occurrence of dense mid-story vegetation cover patches (%) in areas of (a) low, (b) moderate, and (c) high fire severity. The dashed gray line shows the 95th percentile of cumulative patch occurrence. Dense mid-story vegetation patches represented all 10 × 10 m cells with vegetation cover values between 0.5–3.0 m ≥ 20 that shared a straight edge.

Index) was very coarse. The park experienced very heavy rain and a massive erosion event only 5 d after the fire, which we expect to have redistributed many seeds. However, our erosion variable, which relies on a 5-m digital elevation model, would not have captured the micro-scale sites where seeds may be retained or deposited (such as depressions around piles of small rocks).

LiDAR to assess mid-story regrowth

The use of LiDAR to measure forest structure has a history dating back to the 1970s. LiDAR has been shown to be a very accurate tool for measuring and mapping many aspects of vegetation structure (Brosofske et al. 2014), and it has been described as a transformative technology in this respect (Harpold et al. 2015). LiDAR precision was moderate to high in our study with up to 56% of the variance in LiDAR cover explained by field cover. There are many reasons why these relationships were not even higher, including the low pulse density LiDAR data used here, inaccuracies associated with the field surveys and/or vegetation growth between the LiDAR and field surveys. The LiDAR pulse density was sufficient to reliably measure vegetation cover even at a 10 × 10 m cell resolution (80–380 point returns would have been present, even at 40% tree canopy cover) and care was taken during field surveys to correctly assess vegetation cover. Therefore, errors associated with these factors should have been low. It is more likely that vegetation growth in the 11-month interim between the LiDAR and field surveys was responsible for this reduced precision, either via the amount of regrowth (field observations suggest that regenerating seeding's grew up to 1 m during this period meaning that some of the vegetation present between 0.5 and 3.0 m at the time of the LiDAR survey would have exceeded 3.0 m at the time of the field survey and some of the vegetation <0.5 m at the time of the LiDAR survey would have been present between 0.5 and 3.0 m at the time of the field survey) and/or differences in the rate of regrowth (due to fine-scale differences in nutrient availability, topography or microclimate). Given that we observed relatively high R^2 values in our field validation exercise despite these errors, we would argue that our LiDAR data was an apt representation of on-ground vegetation cover.

Despite high precision, accuracy was low, with a consistent underestimation of field cover scores by a factor of ~2. Underestimation of cover by LiDAR has been observed before (Glenn et al. 2011, Wasser et al. 2013). We have applied this methodology to long-unburned eucalypt forests and found only slight underestimation (Price and Gordon 2016). In this study, underestimation is most likely due to the growth of the plants between the time of LiDAR survey and field measurements; i.e., vegetation would have grown thicker and taller and this would have resulted in higher cover scores during the field than LiDAR survey. It might also be because small or pendulous leaves did not trigger a return. This kind of bias presumably varies across plant species and is worthy of further research.

The LiDAR-derived maps present here have potential application to measure current or future fire hazard. Currently, fuel hazard is estimated by one of two methods. Overall fuel hazard is a commonly used visual assessment method, which rates fuel hazard from four strata (surface, near surface, elevated, and bark; McCarthy et al. 1999) at

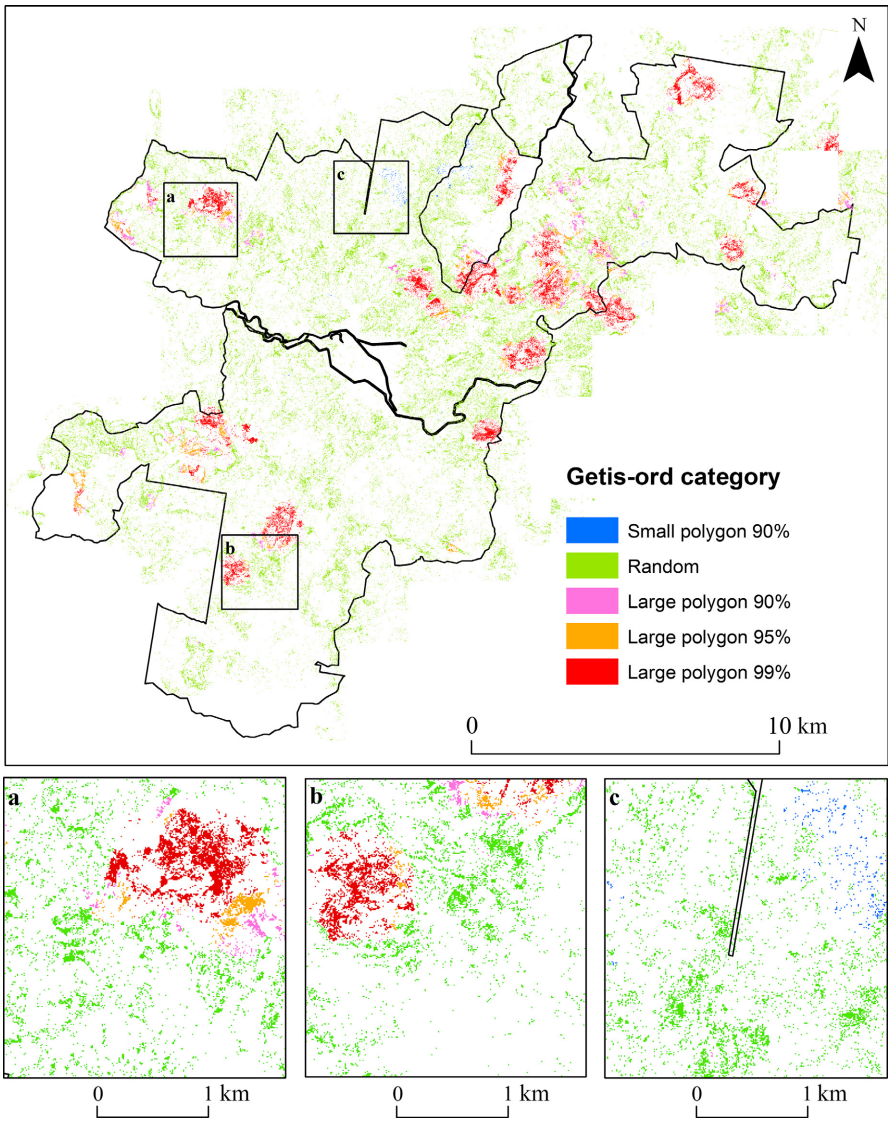

FIG. 6. Map showing spatial clustering of dense mid-story vegetation patches as assessed by the Getis-Ord test statistic. Blue polygons (90th percentile confidence level; small polygon 90%) represent areas where small patches are grouped around other small polygons. Green polygons (random) represent locations where small and large polygons are randomly distributed (i.e., a nonsignificant Getis-Ord test statistic). Pink (90th percentile confidence level; large polygon 90%), orange (95th percentile confidence level; large polygon 95%) and red (99th percentile confidence level; large polygon 99%) polygons represent areas where larger patches are grouped around other larger patches. Dense mid-story vegetation patches represented all 10 × 10 m cells with vegetation cover values between 0.5–3.0 m ≥20% that shared a straight edge. [Color figure can be viewed at wileyonlinelibrary.com]

a single site without spatial information. Fuel hazard maps usually use a combination of vegetation type and time-since-fire (Bradstock et al. 2012, Price et al. 2015). Our study has shown that fuel recovery can vary greatly at small scales suggesting that time-since-fire is not a good surrogate. LiDAR gives a fine-scale and precise measure of elevated and tree cover (though not bark hazard directly), and potentially can measure near-surface cover (material above the ground but <50 cm). LiDAR cannot measure surface fuels (leaf litter, twigs, etc.), but to some extent, these can be predicted from the cover at higher strata (Jakubowksi et al. 2013, Price and Gordon 2016). In any case, in eucalypt forests of southeastern Australia, surface fuel loads generally reach hazardous levels within 3 yr post-fire (Watson 2012) and so can generally be considered to be high for all but recently burned forests. Given the imprecise nature of the overall fuel hazard score, it is likely that LiDAR measures will be equally accurate and more useful given the large spatial areas and fine scale that can be mapped quickly. However, the LiDAR cover values appear to be an underestimate of actual cover, and so would underestimate risk if used

without a correction factor. More research is required into this phenomenon.

Conclusion

Mid-story vegetation regrowth was vigorous but extremely patchy after this fire. Regrowth cover was positively associated with fire severity at each of the spatial resolutions assessed here and was a relatively important biophysical predictor of mid-story cover. Most likely, high-severity fire set the conditions for strong plant growth via breaking seed dormancy, but also by other processes such as reducing competition with trees. Although our main hypothesis was supported, much of the reasons for the vigor of regrowth and its spatial distribution remain unexplained. This suggests that environmental history attributes not measured here (i.e., seed responses of individual plants) strongly influenced the spatial architecture of vegetation regrowth.

Knowledge of vegetation growth following fire is of paramount important for fire management actions because the amount and connectivity of vegetation (i.e., fire fuels) strongly influences rates of fire ignition and spread. Our results suggest that fire hazard will remain relatively low within this landscape if vegetation patches remain isolated from one another. Our results also show the utility of LiDAR data for fuel load and fire hazard mapping over large spatial areas at fine-spatial scales. Therefore, repeated use of LiDAR has great potential as a monitoring tool for investigating the longer term spatiotemporal patterns of post-fire vegetation recovery. This information will be of paramount important for fire management actions that aim to conserve biodiversity but also mitigate human losses due to wildfire.

Acknowledgments

Funding was provided by the New South Wales Office of Environment and Heritage (project number: OEH-178-2015). Andrew Denham provided field assistance and important comments on early manuscript drafts.

Literature Cited

Adams, M., and P. Attiwill. 2011. Burning issues: sustainability and management of Australia's southern forests. CSIRO Publishing, Clayton, Victoria, Australia.

Australian Bureau of Meteorology. 2016. Climate data online. http://www.bom.gov.au/climate/data/

Barton, K. 2011. MuMIn: multi-model inference. R package version 1.0.0. R Foundation for Statistical Computing, Vienna, Austria. http://CRAN.R-project.org/package=MuMIn.

Bazzaz, F. A. 1996. Plants in changing environments: linking physiological, population, and community ecology. Cambridge University Press, Cambridge, UK.

Bradstock, R. A. 2009. Effects of large fires on biodiversity in south-eastern Australia: Disaster or template for diversity? International Journal of Wildland Fire 17:809–822.

Bradstock, R. A., J. E. Williams, and M. A. Gill. 2002. Flammable Australia: the fire regimes and biodiversity of a continent. Cambridge University Press, Cambridge, UK.

Bradstock, R. A., G. J. Cary, I. Davies, D. B. Lindenmayer, O. Price, and R. J. Williams. 2012. Wildfires, fuel treatment and risk mitigation in Australian eucalypt forests: insights from landscape-scale simulation. Journal of Environmental Management 105:66–75.

Brosofske, K. D., R. E. Froese, M. J. Falkowski, and A. Banskota. 2014. A review of methods for mapping and prediction of inventory attributes for operational forest management. Forest Science 60:733–756.

Burnham, K. P., and D. Anderson. 2003. Model selection and multi-model inference: a practical information-theoretic approach. Springer, Berlin, Germany.

Camac, J. S., R. J. Williams, C. H. Wahren, W. K. Morris, and J. W. Morgan. 2013. Post-fire regeneration in alpine heathland: Does fire severity matter? Austral Ecology 38:199–207.

Clarke, P. J., K. J. Knox, R. A. Bradstock, C. Munoz-Robles, and L. Kumar. 2014. Vegetation, terrain and fire history shape the impact of extreme weather on fire severity and ecosystem response. Journal of Vegetation Science 25:1033–1044.

Clarke, P. J., et al. 2015. A synthesis of postfire recovery traits of woody plants in Australian ecosystems. Science of the Total Environment 534:31–42.

Dubayah, R. O., and J. B. Drake. 2000. Lidar remote sensing for forestry. Journal of Forestry 98:44–46.

Fornwalt, P. J., and M. R. Kaufmann. 2014. Understorey plant community dynamics following a large, mixed severity wildfire in a *Pinus ponderosa–Pseudotsuga menziesii* forest, Colorado, USA. Journal of Vegetation Science 25:805–818.

Fu, P., and P. M. Rich. 2002. A geometric solar radiation model with applications in agriculture and forestry. Computers and Electronics in Agriculture 37:25–35.

Gessler, P. E., I. Moore, N. McKenzie, and P. Ryan. 1995. Soil-landscape modelling and spatial prediction of soil attributes. International Journal of Geographical Information Systems 9:421–432.

Getis, A., and J. K. Ord. 1992. The analysis of spatial association by use of distance statistics. Geographical Analysis 24: 189–206.

Gill, A. M. 1975. Fire and the Australian flora: a review. Australian Forestry 38:4–25.

Glenn, N. F., L. P. Spaete, T. T. Sankey, D. R. Derryberry, S. P. Hardegree, and J. J. Mitchell. 2011. Errors in LiDAR-derived shrub height and crown area on sloped terrain. Journal of Arid Environments 75:377–382.

Gonzalez-Olabarria, J. R., F. Rodriguez, A. Fernandez-Landa, and B. Mola-Yudego. 2012. Mapping fire risk in the model forest of Urboin (Spain) based on airborne LiDAR measurements. Forest Ecology and Management 282:149–156.

Gordon, C. E., O. F. Price, E. M. Tasker, and A. J. Denham. 2017. Acacia shrubs respond positively to high severity wildfire: implications for conservation and fuel hazard management. Science of the Total Environment 575:858–868.

Hammill, K. A., and R. A. Bradstock. 2006. Remote sensing of fire severity in the Blue Mountains: influence of vegetation type and inferring fire intensity. International Journal of Wildland Fire 15:213–226.

Harpold, A. A., et al. 2015. Laser vision: lidar as a transformative tool to advance critical zone science. Hydrology and Earth System Sciences 19:2881–2897.

Jakubowksi, M. K., Q. H. Guo, B. Collins, S. Stephens, and M. Kelly. 2013. Predicting surface fuel models and fuel metrics using lidar and CIR imagery in a dense, mountainous forest. Photogrammetric Engineering and Remote Sensing 79:37–49.

Kane, V. R., J. A. Lutz, S. L. Roberts, D. F. Smith, R. J. McGaughey, N. A. Povak, and M. L. Brooks. 2013. Landscape-scale effects of fire severity on mixed-conifer and red fir

forest structure in Yosemite National Park. Forest Ecology and Management 287:17–31.

Kane, V. R., M. P. North, J. A. Lutz, D. J. Churchill, S. L. Roberts, D. F. Smith, R. J. McGaughey, J. T. Kane, and M. L. Brooks. 2014. Assessing fire effects on forest spatial structure using a fusion of Landsat and airborne LiDAR data in Yosemite National Park. Remote Sensing of Environment 151:89–101.

Keeley, J. E. 2009. Fire intensity, fire severity and burn severity: a brief review and suggested usage. International Journal of Wildland Fire 18:116–126.

Keeley, J. E., T. Brennan, and A. H. Pfaff. 2008. Fire severity and ecosystem responses following crown fires in California shrublands. Ecological Applications 18:1530–1546.

Knox, K., and P. Clarke. 2012. Fire severity, feedback effects and resilience to alternative community states in forest assemblages. Forest Ecology and Management 265:47–54.

Levick, S. R., G. P. Asner, and I. P. J. Smit. 2012. Spatial patterns in the effects of fire on savanna vegetation three-dimensional structure. Ecological Applications 22:2110–2121.

Liyanage, G. S., and M. K. J. Ooi. 2015. Intra-population level variation in thresholds for physical dormancy-breaking temperature. Annals of Botany 116:123–131.

McCarthy, G. J., K. G. Tolhurst, and K. Chatto. 1999. Overall fuel hazard guide. Third edition. Department of Sustainability and Environment, Melbourne, Victoria, Australia.

Miller, J. D., and A. E. Thode. 2007. Quantifying burn severity in a heterogeneous landscape with a relative version of the delta Normalized Burn Ratio (dNBR). Remote Sensing of Environment 109:66–80.

Mitchard, E., S. Saatchi, L. White, K. Abernethy, K. Jeffery, S. Lewis, M. Collins, M. Lefsky, M. Leal, and I. Woodhouse. 2012. Mapping tropical forest biomass with radar and spaceborne LiDAR in Lopé National Park, Gabon: overcoming problems of high biomass and persistent cloud. Biogeosciences 9:179–191.

Moore, I., A. Lewis, and J. Gallant. 1993. Terrain attributes: estimation methods and scale effects. Pages 189–214 *in* A. J. Jakeman, M. B. Beck, and M. McAleer, editors. Modeling change in environmental systems. Wiley, London, UK.

Murphy, B. P., A. C. Liedloff, and G. D. Cook. 2015. Does fire limit tree biomass in Australian savannas? International Journal of Wildland Fire 24:1–13.

Nakagawa, S., and H. Schielzeth. 2013. A general and simple method for obtaining R^2 from generalized linear mixed-effects models. Methods in Ecology and Evolution 4: 133–142.

Ooi, M. K. J., R. J. Whelan, and T. D. Auld. 2006. Persistence of obligate-seeding species at the population scale: effects of fire intensity, fire patchiness and long fire-free intervals. International Journal of Wildland Fire 15:261–269.

Ord, J. K., and A. Getis. 1995. Local spatial autocorrelation statistics: distributional issues and an application. Geographical Analysis 27:286–306.

Price, O. F., and C. E. Gordon. 2016. The potential for LiDAR technology to map fire fuel hazard over large areas of Australian forest. Journal of Environmental Management 181:663–673.

Price, O. F., R. Borah, R. Bradstock, and T. Penman. 2015. An empirical wildfire risk analysis: the probability of a fire spreading to the urban interface in Sydney, Australia. International Journal of Wildland Fire 24:597–606.

Purdie, R. W. 1977. Early stages of regeneration after burning in dry sclerophyll vegetation. 2. Regeneration by seed-germination. Australian Journal of Botany 25:35–46.

Purdon, M., S. Brais, Y. Bergeron, and E. van der Maarel. 2004. Initial response of understorey vegetation to fire severity and salvage-logging in the southern boreal forest of Québec. Applied Vegetation Science 7:49–60.

R Development Core Team. 2013. A language and style for computer programing. R Foundation for Statistical Computing, Vienna, Austria.

Rich, P., R. Dubayah, W. Hetrick, and S. Saving. 1994. Using viewshed models to calculate intercepted solar radiation: applications in ecology. American Society for Photogrammetry and Remote Sensing Technical Papers, Bethesda, Maryland, USA.

Tozer, M. G., and R. A. Bradstock. 2003. Fire-mediated effects of overstorey on plant species diversity and abundance in an eastern Australian heath. Plant Ecology 164:213–223.

Turner, M. G., W. H. Romme, and R. H. Gardner. 1999. Prefire heterogeneity, fire severity, and early postfire plant reestablishment in subalpine forests of Yellowstone National Park, Wyoming. International Journal of Wildland Fire 9:21–36.

Wasser, L., R. Day, L. Chasmer, and A. Taylor. 2013. Influence of vegetation structure on lidar-derived canopy height and fractional cover in forested riparian buffers during leaf-off and leaf-on conditions. PLoS ONE 8:e54776.

Watson, P. 2012. Fuel load dynamics in NSW vegetation. Part 1: forests and grassy woodlands. Centre for the Environmental Risk Management of Bushfires, University of Wollongong, Wollongong, New South Wales, Australia.

Zuur, A., E. N. Ieno, N. Walker, A. A. Saveliev, and G. M. Smith. 2009. Mixed effects models and extensions in ecology with R. Springer Science & Business Media, Berlin, Germany.

Supporting Information

Additional supporting information may be found online at: http://onlinelibrary.wiley.com/doi/10.1002/eap.1555/full

Data Availability

Data associated with this paper have been deposited in a Dryad digital repository https://doi.org/10.5061/dryad.jq32s